

# Conical emission, pulse splitting and X-wave parametric amplification in nonlinear dynamics of ultrashort light pulses

Daniele Faccio,<sup>1,\*</sup> Miguel A. Porras,<sup>2</sup> Audrius Dubietis,<sup>3</sup>  
Francesca Bragheri,<sup>4</sup> Arnaud Couairon,<sup>5</sup> and Paolo Di Trapani<sup>1</sup>

<sup>1</sup>*INFM and Department of Physics & Mathematics,  
University of Insubria, Via Valleggio 11, 22100 Como, Italy*

<sup>2</sup>*Departamento de Física Aplicada, ETSIM, Universidad Politécnica de Madrid, Ríos Rosas 21, 28003 Madrid, Spain*

<sup>3</sup>*Department of Quantum Electronics, Vilnius University, Sauletekio Ave. 9, 10222 Vilnius, Lithuania*

<sup>4</sup>*Department of Electronics, University of Pavia, Via Ferrata 1, 27100 Pavia, Italy*

<sup>5</sup>*Centre de Physique Théorique, École Polytechnique,  
CNRS UMR 7644, 91128 Palaiseau Cedex, France*

The precise observation of the angle-frequency spectrum of light filaments in water reveals a scenario incompatible with current models of conical emission (CE). Its description in terms of linear X-wave modes leads us to understand filamentation dynamics requiring a phase- and group-matched, Kerr-driven four-wave-mixing process that involves two highly localized pumps and two X-waves. CE and temporal splitting arise naturally as two manifestations of this process.

PACS numbers: 190.5940, 320.2250

Filamentation of intense light pulses in nonlinear media has attracted much interest ever since first experimental evidences in the early '60's ([1] and references therein). Owing to the very high intensities reached during the process, several nonlinear phenomena, e.g., multiphoton absorption, plasma formation, saturable nonlinear response, stimulated Raman scattering etc., occur in addition to the optical Kerr effect. Indeed, the filament regime is enriched by peculiar phenomena like pulse splitting, self-steepening, shock-wave formation, supercontinuum generation, and conical emission (CE) [2]. In media with normal group velocity dispersion (GVD), no matter if of solid, liquid or gaseous nature, CE accompanies filamentation, producing radiation at angles that increase with increasing detuning from the carrier frequency [3, 4]. In spite of the generality of the process, a clear understanding of the interplay between CE and filament dynamics is still missing. Only recently, Kolesik *et al.* have proposed an interpretation of filamentation dynamics in water on the basis of pulse splitting and dynamic nonlinear X waves at the far field [5], in which the double X-like structure observed in simulated angle-frequency spectra arises from the scattering of an incident field at the two main peaks of the split material response wave.

Originally, CE in light filaments was interpreted in terms of the modulation instability (MI) angle-frequency gain pattern of the plane and monochromatic (PM) modes of the nonlinear Schrödinger equation (NSE) [6, 7]. Measurements at large angles and detunings from the carrier frequency gave in fact results fairly compatible with this interpretation [8, 9]. In the present work, owing to the use of a novel imaging spectrograph technique [3], we have been able to observe for the first time the CE in the region of small angles and detunings. The results clearly indicate a scenario not compatible with the

MI analysis of PM modes. Our description by means of the spectra of the stationary *linear X-waves* supported by the medium, indicates that the strong localization of the self-focused field plays a crucial role in the substantial modification experienced by the MI pattern. We propose a simple picture in which the latter results from the parametric amplification of two weak X-waves by the strong, highly localized pump. Supporting this interpretation, we are able to derive, from the matching condition among the interacting waves, a simple analytical expression [Eq. (4)] that accurately determines the overall CE structure, and predicts also the splitting velocity of the pump wave as a function of the peak intensity reached at collapse.

The experiment was carried out using a 3 cm long cell filled with water as a bulk nonlinear Kerr medium. Beam filamentation was induced by launching 200 fs pulses at carrier wave length 527 nm, delivered from a mode-locked, chirped-pulse regeneratively amplified, Nd:glass laser with a 10 Hz repetition rate (Twinkle; Light Conversion Ltd.). The pulse energy was controlled by use of a half-wave plate and a Glan-Taylor polarizer. A spatial filter guarantees high beam quality before focusing with a  $f = 50$  cm lens placed at 48 cm from the cell input facet, with a beam diameter at half-maximum equal to 100  $\mu\text{m}$ . The output facet is then imaged with a 4- $f$  telescope onto the rear focal plane of the lens ( $f_F = 15$  cm) used to obtain the spatial Fourier transform of the filament generated in the Kerr sample. The input slit of the imaging spectrograph (MS260i, Lot-Oriel) with a high resolution 1200 lines/mm diffraction grating is placed at a distance  $f_F$  from the Fourier lens so as to reconstruct the angle-wavelength ( $\theta$ - $\lambda$ ) spectrum of the filament on a commercial CCD 8-bit camera (Canon), placed at the output plane of the spectrograph. With the change  $\lambda = 2\pi c/(\omega_0 + \Omega)$ , the angle-frequency ( $\theta$ - $\Omega$ ) spectrum can also be obtained,  $\Omega$  being the detuning

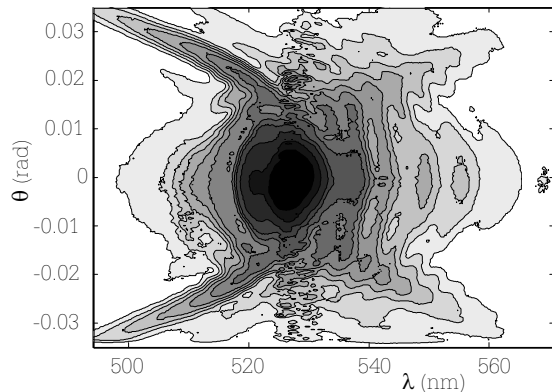


FIG. 1: Measured  $\theta$ - $\lambda$  spectrum for  $E_{\text{in}} = 2 \mu\text{J}$ .

from the carrier frequency  $\omega_0$ . More details of the experimental layout may be found elsewhere [3]. We recorded only single-shot spectra in order to avoid averaging effects due to possible shot-to-shot fluctuations in the input pulse energy. Moreover we highly saturated the central peak of the spectrum so as to highlight the less visible surrounding structure. For input energies  $E_{\text{in}} \lesssim 1.8 \mu\text{J}$ , no CE, or clear X-like features were observed. Figure 1 shows an example of  $\theta$ - $\lambda$  spectrum at  $E_{\text{in}} = 2 \mu\text{J}$ . The CE appears as distinctly separated red- and blue-shifted X-shaped tails. This pattern remains very similar with increasing input energy up to  $E_{\text{in}} \sim 4 \mu\text{J}$ , while further increase produces a slowly deteriorating picture, with a modulated intensity pattern that extends to nearly all recorded values of  $\theta$  and  $\lambda$ . We interpret this deterioration as due to the onset of local breakdown in the water sample.

CE emission is commonly accepted to arise from the interplay of diffraction, dispersion and nonlinear material response, the simplest model that accounts for it being the cubic NSE with normal GVD [6, 7]

$$\frac{\partial A}{\partial z} = \frac{i}{2k_0} \nabla_{\perp}^2 A - \frac{ik_0''}{2} \frac{\partial^2 A}{\partial \tau^2} + i \frac{\omega_0 n_2}{c} |A|^2 A. \quad (1)$$

Here,  $A(x, y, \tau, z)$  is the complex envelope of the wave packet  $E = A \exp(ik_0 z - i\omega_0 t)$  of carrier frequency  $\omega_0$ ,  $\nabla_{\perp}^2 = \partial^2/\partial x^2 + \partial^2/\partial y^2$  is the two-dimensional Laplace operator perpendicular to the propagation direction  $z$ ,  $\tau = t - k_0' z$  is the local time,  $c$  the speed of light in vacuum,  $n_2$  the nonlinear refractive index, and  $k_0^{(m)} \equiv [d^m k(\omega)/d\omega^m]_{\omega_0}$ , where is  $k(\omega)$  the frequency-dependent propagation constant. Mathematically, the  $\theta$ - $\Omega$  spectrum where CE is observable, is directly related to the Fourier spectrum of the envelope. If for instance,  $A(r, \tau, z)$  [ $r = (x^2 + y^2)^{1/2}$ ] is a cylindrical symmetric complex envelope, and  $\hat{A}(K_{\perp}, \Omega, z)$  [ $K_{\perp} = (k_x^2 + k_y^2)^{1/2}$ ] is its spatiotemporal Fourier transform, then the  $\theta$ - $\Omega$  spectrum is given by  $\hat{A}(k_0 \theta, \Omega, z)$ , where  $\theta = K_{\perp}/k_0$  is the propagation angle with respect to the  $z$  axis.

An accepted approach for understanding the structure of the CE relies upon the evaluation of the MI gain profile of the PM modes of the NSE [6]. In Kerr self-focusing media with normal dispersion, the perturbations to a PM mode that grow at maximum rate are those whose spatiotemporal frequencies  $(K_{\perp}, \Omega)$  are related by

$$K_{\perp}(\Omega) = \sqrt{k_0 k_0'' \Omega^2 + 2k_0 \tilde{\beta}}, \quad (\tilde{\beta} > 0), \quad (2)$$

i.e., lie on a hyperbola on the  $K_{\perp}$ - $\Omega$  plane featuring an *angle gap* ( $K_{\perp}$  gap) [6]. In this respect, Luther *et al.* proposed an intuitive picture that assumes the largest MI gain to occur at angles and frequencies fulfilling the linear phase-matching condition of the four-wave mixing (FWM) process supported by the Kerr response [7]. Under this hypothesis, the asymptotic linear approximation  $K_{\perp}(\Omega) \simeq \sqrt{k_0 k_0''} |\Omega|$  was re-obtained, and the observed discrepancies were attributed to the *nonlinear phase shift* produced by the PM mode *on the weak perturbation*.

Preceding experimental observations of CE in borosilicate glass [8] and ethylene glycol [9] were indeed interpreted to present a hyperbolic structure with an angle gap, which was also attributed to the nonlinear phase shift. This trend is also visible in our measurements (Fig. 1) as an intersection of the two X arms at a non-zero angle. If we attempt to fit Eq. (2) (taking  $\tilde{\beta}$  and  $k_0''$  as free parameters) to the experimental data [Fig.2(a), dotted line and closed circles, respectively] we obtain  $k_0'' = 0.053 \pm 0.03 \text{ fs}^2/\mu\text{m}$ , which firmly supports the predictions [7] regarding the asymptotic slope ( $k_0'' = 0.055 \text{ fs}^2/\mu\text{m}$  at 527 nm [10]); however, the angle-gap fitting strongly departs from experimental data in the non-asymptotic region, which strongly calls for a fitting to a hyperbola with opposite curvature, that is, to a hyperbola with a *frequency gap*. This observation advocates a novel interpretation of the origin of CE.

To understand our proposal, note first that the usual MI interpretation of the seemingly angle-gap hyperbolic CE can be equivalently reread in terms of the excitation of a weak, *linear X-wave mode* by a strong, nonlinear PM pump. Indeed, Eq. (2) represents also the  $K_{\perp}$ - $\Omega$  spectrum of an X-wave mode of the medium [11], that is, a diffraction- and dispersion-free pulsed Bessel beam in which cone-angle-induced dispersion [ $\theta(\Omega) \simeq K_{\perp}(\Omega)/k_0$ ] and material GVD balance mutually. The spectrum in Eq. (2) belongs to a wave-mode of carrier frequency  $\Omega_0$  and shortened axial wave vector  $k_0 - \tilde{\beta}$ . In this reading, the excitation of a X-wave mode with angle-gap ( $\tilde{\beta} > 0$ ) is a consequence of the nonlinear phase matching between PM pump and X-wave for maximum efficiency of the interaction: taking into account the nonlinear corrections to the wave vectors of both pump and X-wave, phase matching imposes  $k_0 + \Delta k = k_0 - \tilde{\beta} + 2\Delta k$ , where  $\Delta k = \omega_0 n_2 I/c$  is the *positive* nonlinear phase shift (in self-focusing Kerr medium) for the PM pump of intensity  $I$ , and where  $2\Delta k$  is the corresponding nonlinear correc-

tion to the weak perturbation [8, 9], leading immediately to  $\tilde{\beta} = \omega_0 n_2 I / c > 0$  (as predicted by the standard MI analysis [6]).

We also note that a medium with GVD [ $k(\Omega) = k_0 + k'_0 \Omega + k''_0 \Omega^2 / 2$ ] supports more general X-wave modes with strengthened and shortened wave vectors ( $\tilde{\beta}$  negative and positive), as well as shifted carrier frequency  $\omega_0 + \tilde{\Omega}$ , their most general  $K_\perp - \Omega$  spectrum being expressed by [11]

$$K_\perp(\Omega) = \sqrt{k_0 k''_0 (\Omega - \tilde{\Omega})^2 + 2k_0 \tilde{\beta}}, \quad (\tilde{\beta} \gtrless 0). \quad (3)$$

Their phase and group velocities are given by  $v^{(p)} = (\omega_0 + \tilde{\Omega}) / [k(\tilde{\Omega}) - \tilde{\beta}]$  and  $v^{(g)} = 1 / k'(\tilde{\Omega})$ , respectively, which can take both subluminal and superluminal values. Equation (3) describes a two-parameter family of hyperbolas, sharing the same asymptotic slope  $\sqrt{k_0 k''_0}$ , but admitting angle gaps ( $\tilde{\beta} > 0$ ) and frequency gaps ( $\tilde{\beta} < 0$ ), as well as positive and negative frequency shifts  $\tilde{\Omega}$ . X-wave spectra appear then as a suitable tool for the description of the CE features.

The apparent frequency-gap hyperbolic form of the observed CE, and the actual absence of such a gap, suggest that the CE cannot be described in terms of a single X-wave. This leads us to interpret the two observed X tails as belonging to two different X waves both featuring frequency gaps, and proceed to fit Eq. (3) with two independent sets of parameters  $\tilde{\Omega}$  and  $\tilde{\beta}$  (and  $k''_0 = 0.056 \text{ fs}^2 / \mu\text{m}$ ) to the experimental data. This procedure also finds motivation in the X-X structure of the numerically evaluated angular spectra of light filaments in water, which was interpreted to be a consequence of pulse splitting on X-wave generation [5]. Fittings with  $\tilde{\Omega} = +0.33, -0.33 \text{ fs}^{-1}$  and  $\tilde{\beta} = -2.2, -2.2 \text{ mm}^{-1}$  (dashed and continuous lines, respectively) reproduce accurately the structure of the CE [Fig. 2(a)]. The interpretation in term of X-waves leads moreover to suspect the existence of two additional, not yet observed X arms in the  $K - \Omega$  spectrum at wavelengths 450 and 635 nm [Fig. 2(a)].

To verify this prediction, we performed additional measurements with a lower resolution, 300 lines/mm diffraction grating in order to cover a wider spectral region, as shown in Fig. 2(b). Alongside the central tails (around 527 nm), we clearly observe the generation of new frequencies in the vicinity of 450 and 635 nm, as expected. The reduced visibility of the red tail at 635 nm can be attributed to the stronger linear absorption at this wavelength. In fact, we had to increase the input pulse energy up to  $E_{\text{in}} = 3 \mu\text{J}$  in order to enhance the overall intensity of the new tails.

The question then arises of the mechanism responsible for the described spectral structure. Here we propose that the double X-like CE is a result of a nonlinear FWM interaction—the lowest order process supported by the nonlinear Kerr response—in which two signal and idler X-waves experience a parametric amplification by a strong, *highly localized* (i.e., non PM) pump. If as

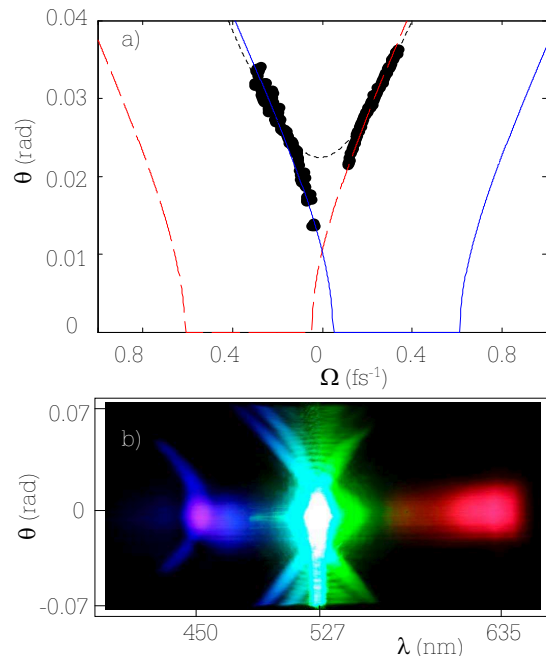


FIG. 2: (Color online) a) Closed circles:  $\theta - \Omega$  distribution of peak fluence in Fig. 1; dotted line: best fit of the entire set of experimental data with Eq. (2); red-dashed line: best fit of the  $\Omega < 0$  data with with Eq. (3); blue-full line: best fit of the  $\Omega > 0$  data with with Eq. (3) b) Experimentally measured  $\theta - \lambda$  spectrum for  $E_{\text{in}} = 3 \mu\text{J}$ , showing the Stokes and anti-Stokes sidebands.

consistently with the self-focusing dynamics, we consider a strongly localized pump rather than a PM wave, it is expected that nonlinear phase modulation does not influence significantly an extended object such an X-wave mode, whose axial wave vector is solely determined by its cone angle, that is, by its weak, longstanding tails far from the pump. In fact, in the X-wave the energy does not flow along the axial direction, but along a conical surface, which prevents pump-induced cross-phase accumulation to take place.

Under this assumption, phase matching between a localized pump and a single X-wave at same frequency  $\omega_0$  would require  $k_0 + \Delta k = k_0 - \tilde{\beta}$ , a condition that contrarily to the case of a PM pump, is satisfied by a frequency-gap X-wave mode ( $\tilde{\beta} = -\Delta k < 0$ ). More generally, if  $k = k_0 + \Delta k$  is the nonlinear pump wave number, and  $k_{s,i} = k(\tilde{\Omega}_{s,i}) - \tilde{\beta}_{s,i}$  are two, signal and idler, X wave numbers, where  $k(\tilde{\Omega}_{s,i}) = k_0 + k'_0 \Omega_{s,i} + k''_0 \Omega_{s,i}^2 / 2$ , and  $\Omega_{s,i}$  are their carrier frequency shifts, the conditions of energy and momentum conservation,  $\tilde{\Omega}_s = -\tilde{\Omega}_i$  and  $2k = k_s + k_i$ , for maximum efficiency of a FWM process involving two (degenerate) highly localized pumps and the signal and idler X waves, leads to the relation  $\tilde{\beta}_s + \tilde{\beta}_i - k''_0 \Omega_{s,i}^2 = -2\Delta k$ . Among all possible couples of X-wave modes satisfying this relation, those whose spectra cross the pump, located around  $\Omega = 0, K_\perp = 0$ , are

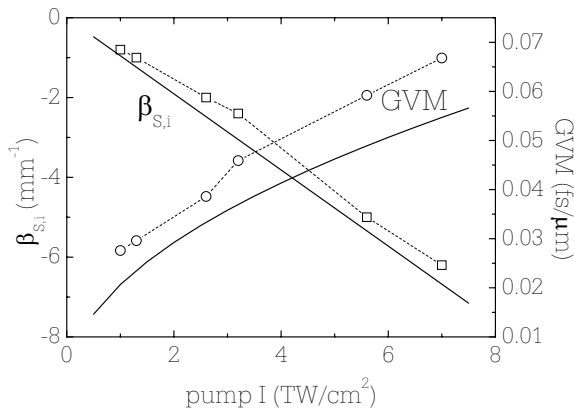


FIG. 3: Left: Values of  $\tilde{\beta}_{s,i}$  obtained from X-wave fitting to the numerical  $K_{\perp}$ - $\Omega$  spectra for increasing pump intensities  $I$  (open squares), and prediction of Eq. (4) (solid curve). Right: GVM between the splitting pulses obtained from direct space-time numerical simulation (open circles), and between the X-waves as given by  $2\sqrt{k_0''\omega_0 n_2 I/c}$  (solid curve).

the most energetically favored, since these X-waves will not need to grow from noise, but from the more effective pump self-phase modulation. This condition was also found in [12] to result in the largest gain in the case of a single X wave excited by a travelling pump. The X-wave-pump crossing condition leads, from Eq. (3), to  $\tilde{\beta}_{s,i} = -k_0''\tilde{\Omega}_{s,i}^2/2$ , and then, on account that  $\Delta k = \omega_0 n_2 I/c$ , to

$$\tilde{\beta}_{s,i} = -\omega_0 n_2 I/2c. \quad (4)$$

Accordingly, the two X-waves will present symmetrically shifted carrier frequencies  $\tilde{\Omega}_{i,s} = \pm\sqrt{\omega_0 n_2 I/c k_0''}$ , and frequency-gaps of width  $2|\tilde{\Omega}_{i,s}|$ , from  $\Omega = 0$  towards the Stokes and anti-Stokes bands, as observed in the experiment.

Eq. (4) predicts also a precise dependence of the whole CE structure on the pump intensity  $I$ , whose validity we have tested numerically. We solved the NSE (1) with  $k_0'' = 0.056 \text{ fs}^2/\mu\text{m}$ ,  $n = 1.33$  and  $n_2 = 1.6 \times 10^{-16} \text{ cm}^2/\text{W}$ , for an input 200 fs-long, 100  $\mu\text{m}$ -wide (FWHM) Gaussian wave packet. Since CE is seen to develop explosively at the collapse, we identified the pump intensity  $I$  with the absolute peak intensity reached during propagation. In order to attain different values of this intensity without changing the rest of parameters, we added to the second member of the NSE (1) the nonlinear dissipation term  $-\beta^{(K)}|A|^K A/2$ , with  $K = 3$  (three-photon absorption at 527 nm in water), and with  $\beta^{(K)}$  ranging from  $1.2 \times 10^{-23}$  to  $8 \times 10^{-25} \text{ cm}^3/\text{W}^2$ . The  $K_{\perp} - \Omega$  spectra obtained numerically are symmetric with respect to  $\Omega = 0$  due to the approximations involved in the NSE, and present a nearly invariant X-X structure beyond the collapse point (in spite of the quickly decreasing peak intensity  $I$ ), with one tail of each X wave nearly passing through  $\Omega = 0$ , as observed experimentally. The

spectrum at 3 cm from the input plane was then easily fitted with two, signal and idler, material X-waves modes crossing  $\Omega = 0$  [i.e., with  $k_0'' = 0.056 \text{ fs}^2/\mu\text{m}$ , and with  $\tilde{\Omega}_{s,i} = \pm(-2\tilde{\beta}_{s,i}/k_0'')^{1/2}$ ],  $\tilde{\beta}_{s,i}$  being then the only one free parameter. Figure 3 shows the values of  $\tilde{\beta}_{s,i}$ , obtained from the best fits to the spectra, versus pump intensity  $I$  (open squares). The excellent agreement with the predicted  $\tilde{\beta}_{s,i}$ - $I$  dependence in Eq. (4) (solid line) strongly supports the FWM analysis.

Extending further our interpretation, we conjecture that the well-known phenomenon of pulse temporal splitting in filamentation with normal GVD, usually described from a purely temporal perspective, is a consequence of higher-order matching among the interacting waves—in our case, of *group matching*. Indeed, the zero-order, phase-matching condition (4) entails that the two X-waves must travel at different group velocities  $v_{s,i}^{(g)} = 1/k'(\Omega_{s,i}) = 1/[k_0' + k_0''\Omega_{s,i}]$ , and therefore split apart in time one from another with a group velocity mismatch (GVM)  $1/v_s^{(g)} - 1/v_i^{(g)} = 2k_0''|\tilde{\Omega}_{s,i}| = 2\sqrt{k_0''\omega_0 n_2 I/c}$  proportional to the square root of the pump intensity. Group matching among the interacting waves is then better attained if the two pump waves, breaking their initial degeneracy, split also to co-propagate with the X-waves. In this view, pulse splitting is not a mere collapse-arresting mechanism [7], which further determines, taken it for granted, the generation of two X-waves [5]; instead, pulse splitting emerges here as a particular feature of the phase and group matched wave configuration most favored by the FWM nonlinear interaction inherent to the Kerr NSE dynamics. In other words, X-wave instability or parametric amplification, and splitting instability are not independent phenomena, but two aspects of the same process. To sustain this hypothesis, we have evaluated the GVM of the split pumps in the same numerical simulations as in the preceding paragraph. To do so, we plotted the temporal profiles at different propagation distances beyond collapse, and obtained the GVM as the slope of a linear fitting to the delay between the two temporal peaks versus propagation distance. Figure 3 shows that the pump GVM (open circles) does not depart more than 10 percent from the predicted X-wave GVM (solid curve), and that both follow a similar dependence with the square root of the intensity  $I$  at collapse.

In summary, our experiments demonstrate that CE emission in the angular spectrum of filaments is not interpretable in the frame of MI of PM modes of the NSE. Strong localization of the self-focusing pulse substantially modifies the MI pattern, which finds accurate description in terms of linear X-wave modes of the medium, and simple explanation as a result of a dominant, phase-matched FWM mixing process supported by the NSE dynamics between two highly localized, strong pump waves and two amplifying weak X-waves. Pulse temporal splitting emerges in this model as the necessary temporal dynam-

ics for preserving group matching among the interacting waves.

---

\* Electronic address: danielle.faccio@uninsubria.it

- [1] J. Marburger, *Progr. Quant. Electron.* **4**, 35 (1975).
- [2] A. Gaeta, *Science* **301**, 54 (2003).
- [3] D. Faccio, P. Di Trapani, S. Minardi, A. Bramati, F. Bragheri, C. Liberale, V. Degiorgio, A. Dubietis, and A. Matijosius, *J. Opt. Soc. Am. B* **22**, 862 (2005).
- [4] E. Nibbering, P. Curley, G. Grillon, B. Prade, M. Franco, F. Salin, and A. Mysyrowicz, *Opt. Lett.* **21**, 62 (1996).
- [5] M. Kolesik, E.M. Wright, and J.V. Moloney, *Phys. Rev. Lett.* **92**, 253901 (2004).
- [6] L.W. Liou, X.D. Cao, C. McKinstrie, and G.P. Agrawal, *Phys. Rev. A* **46**, 4202 (1992).
- [7] G. Luther, J. Moloney, A. Newell, and E. Wright, *Opt. Lett.* **19**, 862 (1994).
- [8] R. Alfano and S. Shapiro, *Phys. Rev. Lett.* **24**, 584 (1970).
- [9] Q. Xing, K. Yoo, and R. Alfano, *Appl. Opt.* **32**, 2087 (1993).
- [10] A. Van Engen, S. Diddams, and T. Clement, *Appl. Opt.* **37**, 5679 (1998).
- [11] M.A. Porras and P. Di Trapani, *Phys. Rev. E* **69**, 066606 (2004).
- [12] C. Conti, *Phys. Rev. E* **70**, 046613 (2004).